Comparison of Emissions from a Transmission Line on a CISPR 25 Bench Setup and Test Vehicle

Ch Umer Sajjad
Department of Electronic Engineering
University of York
York, England
chumer.sajjad@york.ac.uk

J. F. Dawson
Department of Electronic Engineering
University of York
York, England
john.dawson@york.ac.uk

Ayhan Gunsaya
In-House Electronics
Ford Motor Company
England
agunsaya@ford.com

Andy Marvin
Department of Electronic Engineering
University of York
York, England
andy.marvin@york.ac.uk

***Abstract*—Compliance with radiated emission requirements is one of the biggest challenges faced by the automotive industry. The CISPR 25 bench test is one of the initial test methods that can help the industry to estimate the emissions in the real vehicle but this is hampered by lack of strong correlation. In this paper, a one tenth scale model approach is used to observe the behavior of emissions from a simple transmission line source placed first on a test bench and later in a vehicle.**

Keywords—CISPR-25, Electromagnetic Emissions, Automotive EMC

I. Introduction

In recent years, electromagnetic fields inside and outside automobiles have increased significantly due to electrification, autonomous driving, increased use of PWM control of high power loads and migration from linear regulators to switched mode power supplies for increased efficiency. Among these changes, ensuring EMC performance is becoming increasingly important. In general, higher costs are incurred if problems occur later in the product design process. Therefore, early EMC performance prediction and design is very important. As a typical test for checking the radiated emission characteristics of automotive parts, the absorber-lined shielded enclosure (ALSE) method of the International Special Committee on Radio Interference 25 (CISPR 25) is used.

Since the introduction of the CISPR 25 standard in 1995, the complexity of electronic control units (ECUs) and wire harnesses has increased significantly. Today's control units not only use several different bus systems, but also some of the same type in parallel. However, the measurement settings specified in the standard have hardly changed [1]–[3]. To measure the radiated emissions of a component, CISPR-25 requires that it is connected to the load simulator via a cable (test harness). This test covers the frequency range from 150 kHz to 4. 9 GHz [4], and includes both bench and in-vehicle tests.

Because of external interference, the performance of radio receivers, such as the broadcast radio, can be degraded. The frequencies used range from 150 kHz to 250 MHz (typically car radios can be tuned to LW, MW, FM and DAB broadcast signals). For that frequency range the automotive industry uses CISPR 25, both for component level and vehicle level assessments. For this research, we elected to use a one tenth scale model because we had limited access to a vehicle size EMC chamber. The frequencies used are therefore scaled up by a factor of ten to give the same electrical size in wavelengths for the model as the real vehicle. For the vehicle, a 6.4 m long simplified van model (basic geometry of the vehicle), scaled to 640 mm, is used for the testing. These models are simulated using CST Microwave Studio [5] FIT time domain solver, and measured in a reverberation chamber. The scaled dimensions and frequency values are used throughout the remainder of this paper.

In this paper we concentrate on how the behaviour of a single wire transmission line behaves in a range of scenarios in terms of the energy propagation on the line and radiation from the line. In Section II we describe the scaled models used, then in Section III we describe the measurements and numerical simulations performed, and in Section IV we present the results, before drawing conclusions.

II. Scaled Models

There are four Scaled models that are used in this paper.

1. Standard CISPR 25 bench set-up with 1.5 m transmission line, scaled to 150 mm (Fig. 1).
2. CISPR 25 1.5 m line, scaled to 150 mm, but on the floor of the model van with no body present (Fig. 2).
3. A modified CISPR 25 setup but with a 4.64 m transmission line, scaled to 464 mm, on the floor of the model van with no body present (Fig. 3).
4. As 3 above but with the model van body present (Fig. 4).

A 50 Ω source or termination is used at each end of the transmission line to facilitate simple measurements using a network analyser. Port 1 is placed at the near end of the transmission line as seen in the figures, whereas Port 2 is placed at the far end. We write the port number on the top of the boxes in the physical model. Each transmission line is connected to a panel mounting SMA socket mounted on the box, with the socket facing inward. In the CST model we model the coaxial structure of the connector and place a waveguide port, with a 50 Ω normalising impedance, inside each box. Both boxes are placed directly on the ground plane, which has holes large enough to connect cables to the SMA connectors inside the boxes. Cables then emerge below the ground-plane to minimise their interaction with the transmission line.

This research is Funded by Ford Motor Company under the 2018-6040R URP award: Developing alternatives to vehicle EMC testing.

978-1-7281-5579-1/20/$31.00 ©2022 IEEE

In the numerical model all of the metal parts are modelled as perfect electrical conductors (PECs). The only other material is the lossy PTFE (Polytetrafluoroethylene) used in the connector part. Absorbing boundary conditions are used.

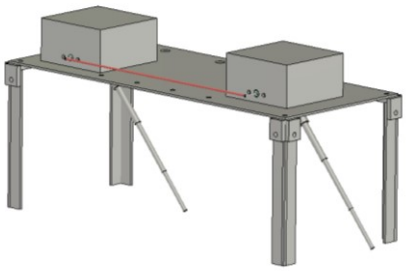

Fig. 1. 1/10th scale Model of Standard CISPR 25 bench setup with 150 mm transmission line.

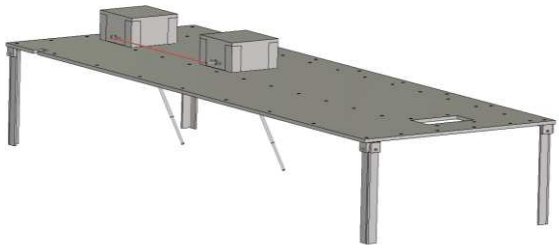

Fig. 2. CISPR 25 "bench setup"on the floor of the van model.

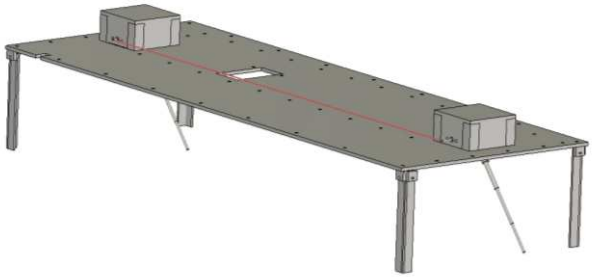

Fig. 3. Van floor with boxes connected by the 464 mm long transmission line.

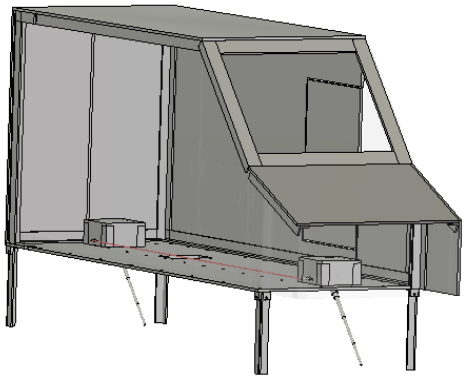

Fig. 4. Van floor and body with 464 mm long transmission line with side of van hidden to show boxes inside.

III. Measurement and Simulation Setup

A. Reverberation chamber measurements

The measurements presented in this paper were all conducted in a reverberation chamber of dimensions 4.7 m long, by 3.0 m wide, by 2.7 m high, with a 2 m diameter stirrer. Coupling measurements were taken using a vector network analyser (VNA). For the chamber coupling measurements 100 stirrer positions over one stirrer rotation were used to compute the radiated power from the model. It was observed that the stirrer position did not noticeably affect the line S-parameters so only a single stirrer position is reported for line S-parameters.

Fig. 5 shows the model CISPR test bench placed on a polystyrene block in the reverberation chamber. The transmission line port connections to the chamber access panel can be seen. Fig. 6 shows the model van floor in the chamber. The chamber reference antenna [6] can be seen on the floor.The receiving antenna is of identical type and is mounted on the wall behind the stirrer.

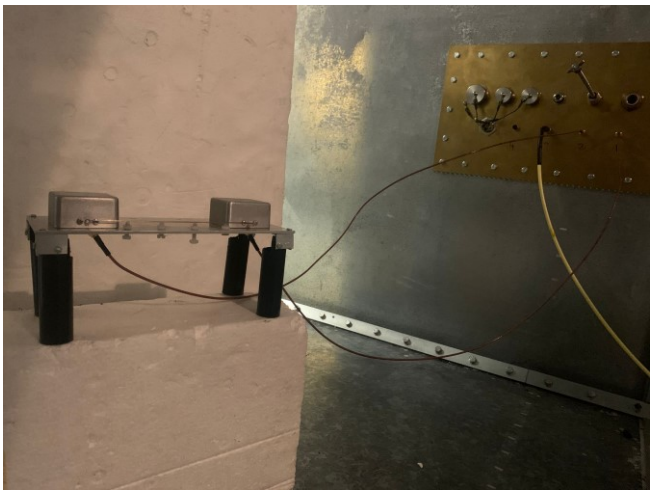

Fig. 5. CISPR 25 bench model in the reverberation chamber showing connecting cables to transmission line ports connected to chamber panel

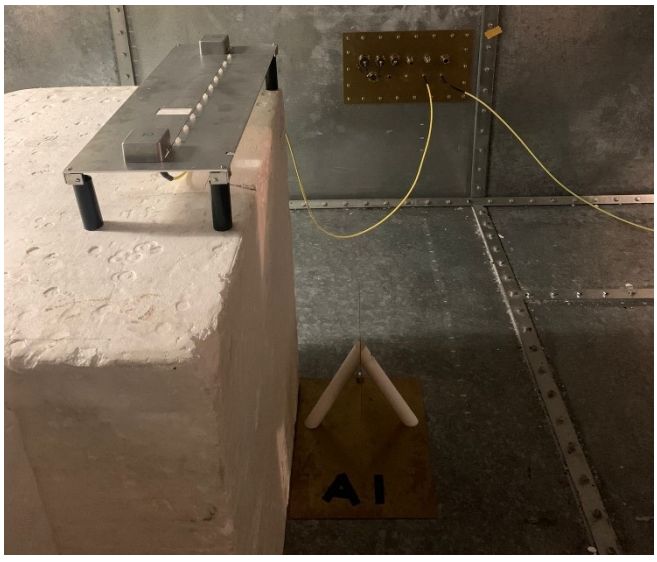

Fig. 6. Van model floor with 464 mm line in the reverberation chamber showing chamber reference antenna on floor.

B. Simulation setup

The two line ports were each excited in separate simulations and the radiated power was recorded. In order to constrain storage usage, full radiation patterns were recorded at a small number of frequencies, whilst to obtain a full frequency sweep estimation of total radiated power a set of 64 far-field probes uniformly placed in orthogonal pairs on the surface of a sphere as in [7], at 10 m from the centre of the ground plane were used.

IV. Results and Discussion

A. Energy decay in simulation

In any time-domain simulation, the energy within the simulation must be allowed to decay sufficiently in order to achieve a reliable result in the frequency domain. A decay of 20 dB can give reasonable results but greater levels of decay can be desirable to see low level features in the frequency response. We found the energy decay curves gave an interesting insight into the behaviour of the models.

Fig. 7 shows Energy Decay for the 150 mm lines on the CISPR bench model and van floor models. It can be seen that the energy decays in steps corresponding to the delay time of the transmission line, which are caused by energy in propagating pulse being absorbed each time it meets the load at the end of the line. There is a slower decay between steps which must be due to radiated energy lost in the absorbing boundary conditions of the model as there is no loss in the PEC parts. It can be seen that there is little difference between the CISPR bench and van floor.

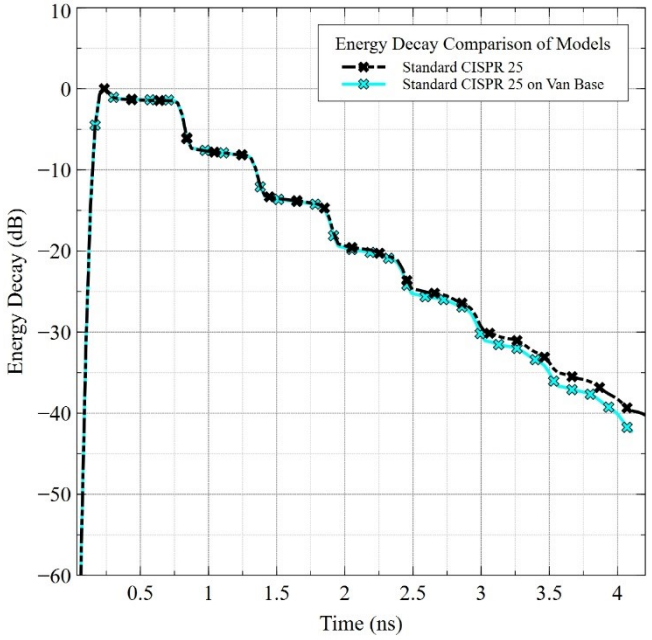

Fig. 7. Energy Decay for the 150 mm lines on the CISPR bench model and van floor models

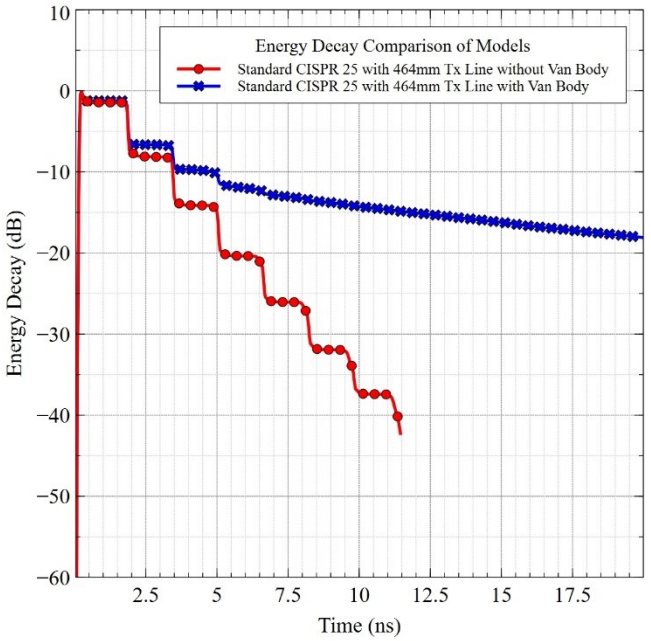

Fig. 8. Energy Decay for 464 mm line on the van floor with and without the van body.

Fig. 8 shows the energy decay for the 464 mm transmission line on the van floor with and without the van body. With no van body the decay curve is similar to those in Fig. 7, except that the time between steps in the energy curve is longer, in proportion to the longer line length. When the van body is present the steps are smaller in size and the curve becomes smooth after about 5 ns. This suggests that the majority of the energy in the problem space is now contained in the van body and escapes slowly through the apertures compared to the rate of energy loss when the body is not present. The fact that the steps can barely be seen after 5 ns suggests the energy stored in space in the body is larger than that in the fields around the line. The van body is giving some reverberant enhancement of the internal fields. This is likely to result in a significant difference in the fields around the line compared to the CISPR bench and van floor cases.

B. Transmission line S-Parameters:

The S-parameters of the transmission line give an important view of its operation and any interaction with features such as the ground-plane, enclosures, and van body in the model, also any interaction with the reverberation chamber in the measurements.

Fig. 9 shows that the S-parameters of the 150 mm line are not significantly affected by the difference between the CISPR bench and van floor. The periodicity in the frequency domain is approximately 1 GHz which is as expected for a 150 mm line, and the end to end loss is partly due to mismatch (the line impedance is computed to be 192 Ω), and partly due to energy radiated from the line.

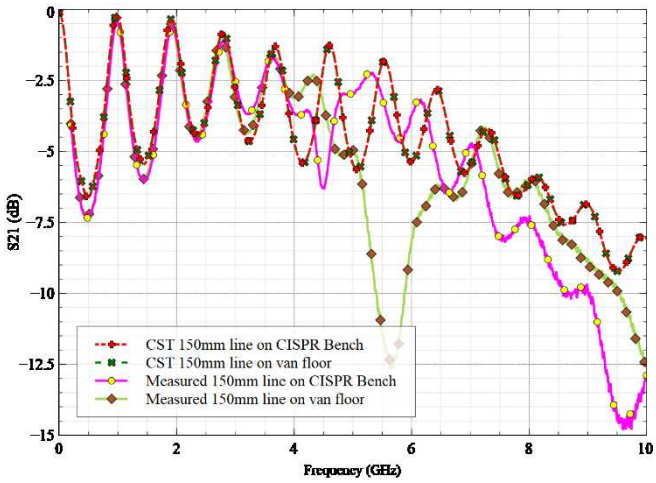

Fig. 9. Comparison of S21 for the 150 mm line on the CISPR bench and van floor, simulated with CST and measured

Fig. 10 shows that the S-parameters of the 464 mm line are similar with and without the van body up to 5 GHz. Again the periodicity corresponds to the line length. However, in the case where the van body is present some additional structure can be seen in the S-parameters due to coupling with van body modes. The additional structure is quite small.

In both Fig. 9 and Fig. 10 the measured data diverges from the model at around 5 GHz, further work is required to determine the cause.

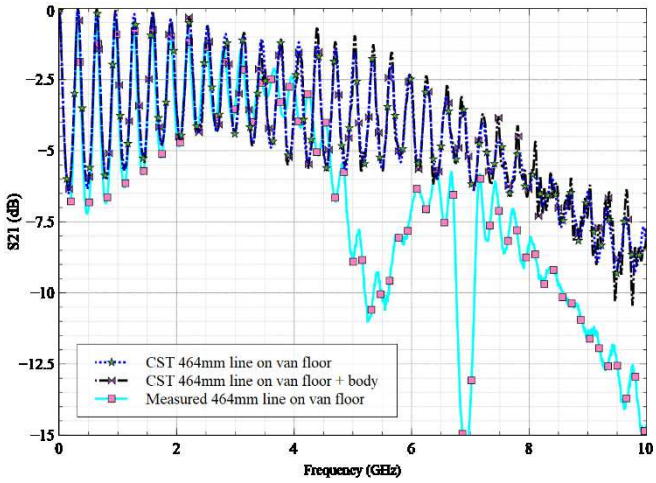

Fig. 10. Comparison of S21 for the 464 mm line with and without Van body

C. Radiation pattern

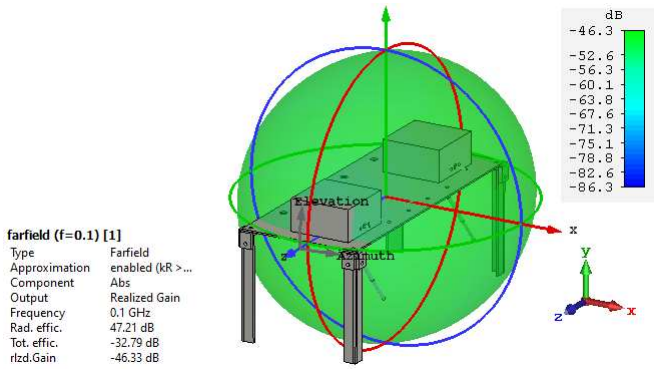

Fig. 11. Far Field of 150mm line on CISPR 25 bench at 100 MHz

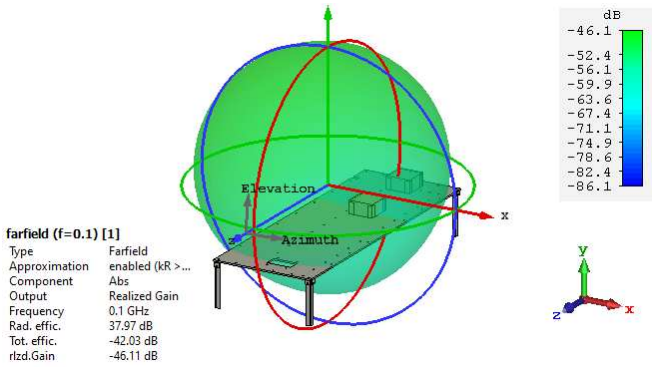

Fig. 12. Far Field of 150 mm line on van floor at 100 MHz

Fig. 11 and Fig. 12 show the radiation pattern of the 150 mm line at 100 MHz (equivalent to 10 MHz at full scale) on the CISPR bench and van floor. Both show a near isotropic pattern, with a realised maximum gain of about -46 dB. This is as expected for an electrically small (1/20th wavelength) lossy antenna.

Fig. 13 and Fig. 14 show the radiation pattern of the 464 mm line at 100 MHz on the van floor without and with the van body. A more obvious directivity, with backward radiation from the near end, as expected, is visible The maximum realised gain is about -43dB for the line on with no van body. When the van body is present there is a similar directivity but a greatly reduced gain of about -63dB.

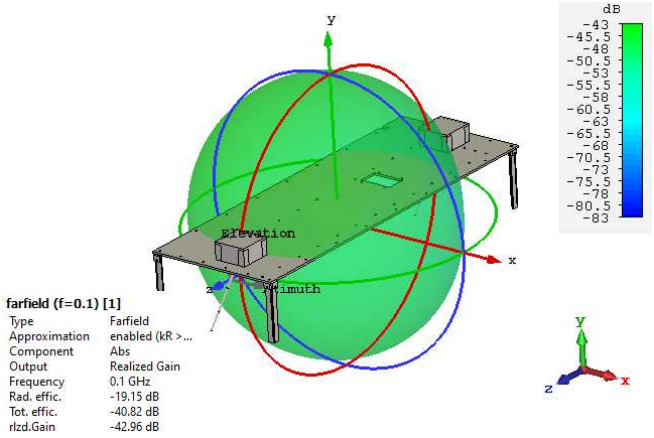

Fig. 13. Far field of 464 mm line on van floor at 100 MHz

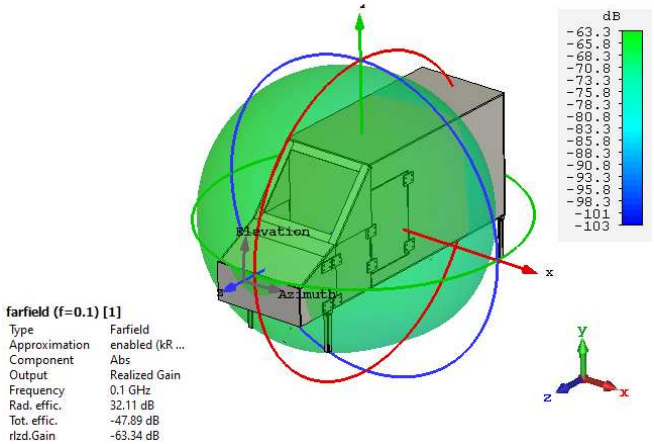

Fig. 14. Far field of 464 mm line on van floor with van body at 100 MHz

At 2.5 GHz, which is representative of the upper range for DAB radios when scaled to 250 MHz in the full size case, the patterns are rather more complex and different. This can be seen in the patterns of Fig. 15 to Fig. 18. Whilst the 150 mm line exhibits a maximum realized gain of about −5 dB; and the longer line has a slightly larger value of −1.6 dB on the van floor, the presence of the van body still reduces the realized gain a little to about −3.5 dB.

As expected, the pattern complexity and gain carry on increasing with frequency as can be seen in Fig. 19

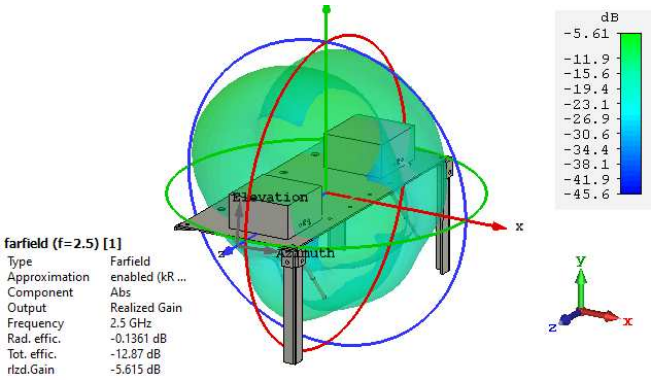

Fig. 15. Far Field of 150 mm line on CISPR 25 bench at 2.5 GHz

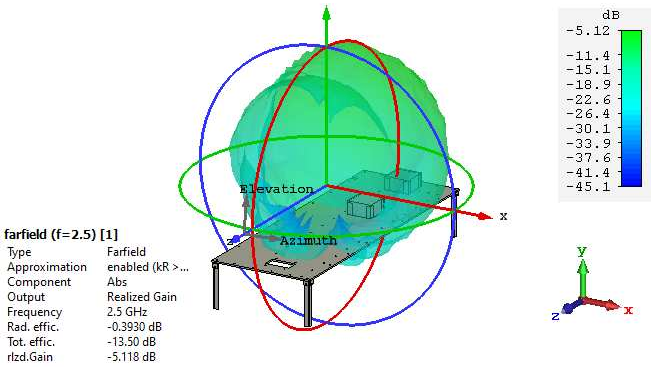

Fig. 16. Far Field of 150 mm line on van floor at 2.5 GHz

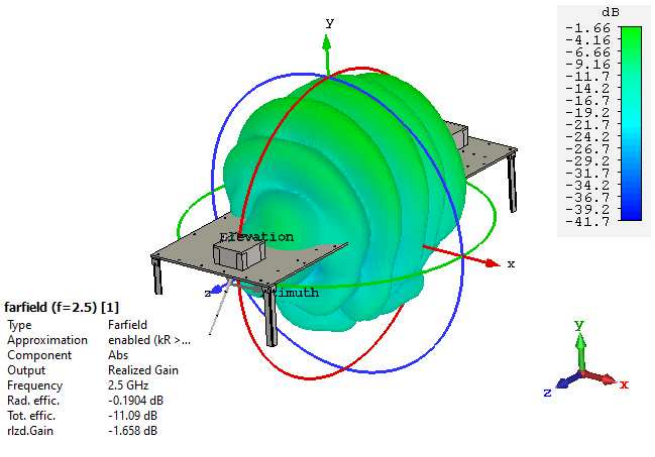

Fig. 17. Far Field of 464 mm line on van floor at at 2.5 GHz

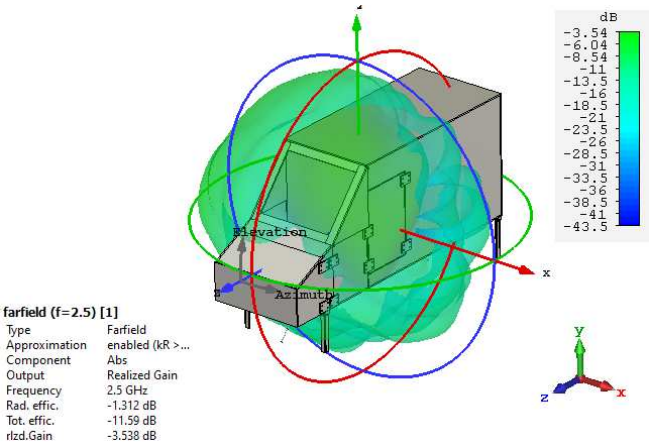

Fig. 18. Far Field of 464 mm line on van floor with van body at 2.5 GHz

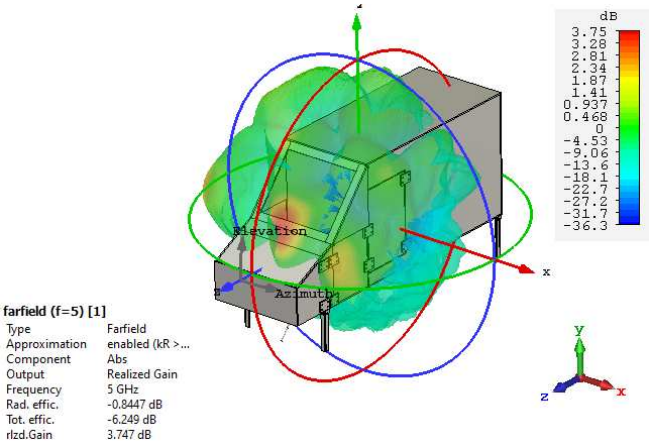

Fig. 19. Far Field of 464 mm line on van floor with van body at 5 GHz.

D. *Total radiated power*

Using the 64 far field probes surrounding the model we were able to estimate the total radiated power of each scenario. Using reverberation chamber measurements, we were able to measure the total radiated power. The results are plotted as average radiation efficiency which is the ratio of the total radiated power to the incident power on the transmission line. This is equal to the average realized gain.

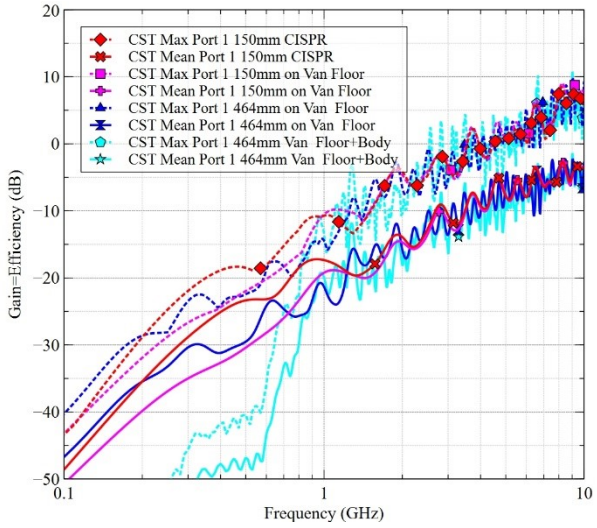

Fig. 20. Mean and Max realised gain for excitation at port 1 for simulated models

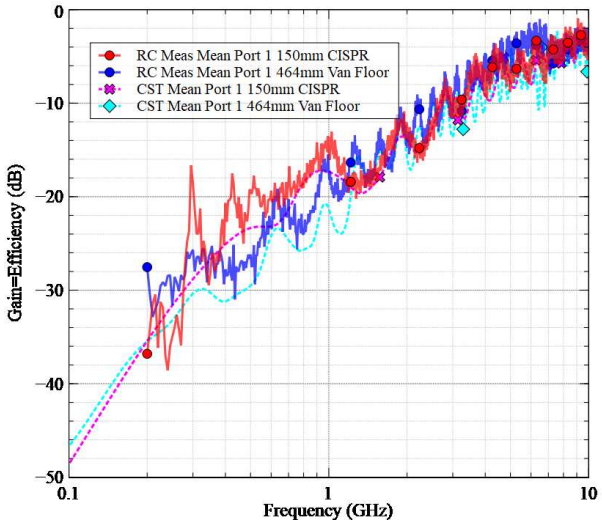

Fig. 21. Mean realised gain from CST simulation vs RC measurement

Fig. 20 shows the average realised gain (average radiation efficiency) and the maximum realised gain for the different scenarios. It can be seen that the average radiation efficiency seen for all the scenarios is comparable at frequencies above 1 GHz. Below 1 GHz it can be seen that the presence of the vehicle body provides a substantial shield effect reducing the average radiation efficiency and maximum gains. It can also be seen that the maximum value of the realised gain seen by the 64 probes is about 10dB above the mean. Fig. 21 compares the simulated and measured mean realised gain (radiation efficiency), which show a good correspondence above 1 GHz, with some greater deviation below due to the worsening performance of the reverberation chamber below 1 GHz.

V. Conclusions and Further Work

This preliminary work has shown that the total radiated power from a transmission line with lossy loads, as surrogate for a cable loom, remains largely constant regardless of the line length and ground plan on which it is mounted. However, the presence of a vehicle body provides some reduction (shielding) at lower frequencies. There seems to be about 10dB difference between the mean and maximum gain of the radiation pattern and the pattern does differ with different length lines and different ground planes once the structure becomes a comparable to the wavelength. This is suspected as a significant contributor to the differences observed in practice between bench and whole vehicle measurements, along with the body shielding effect at lower frequencies.

The cable S-parameters are largely unaffected by the size of the ground plane (presuming it to be away from edges of the plane) in the CST model results, though some structure from the resonant modes of the van body can just be seen at higher frequencies. The measured S-parameters diverge from the model above 5 GHz and further work is needed to determine the cause of this.

In future work we aim to conduct further measurements in an anechoic environment, to better replicate CISPR measurements, and supplement this with modeling. We will also investigate more typical transmission line routes, and the effect of line resonances when the terminations are low loss.

References

[1] T. H. Hubing, “Module-level characterization for vehicle-level emissions modeling,” in *2010 Asia-Pacific International Symposium on Electromagnetic Compatibility*, 2010, pp. 680–682.

[2] A. Radchenko, V. V. Khilkevich, N. Bondarenko, D. Pommerenke, M. Gonser, J. Hansen, and C. Keller, “Transfer Function Method for Predicting the Emissions in a CISPR-25 Test-Setup,” *IEEE Transactions on Electromagnetic Compatibility*, vol. 56, no. 4, pp. 894–902, 2014.

[3] J. Schabel, M. Zerrer, M. Kull, M. Beltle, and S. Tenbohlen, “Methods for Investigating Influence Parameters in the Measurement Setup for Radiated Emissions according to CISPR 25,” in *2021 IEEE International Joint EMC/SI/PI and EMC Europe Symposium*, 2021, pp. 110–114.

[4] *Vehicles, Boats and Internal Combustion Engines - Radio Disturbance Characteristics - Limits and Methods of Measurement for the Protection of On-board Receivers," CISPR 25, Ed. 5.0, 2021.* IEC Test Standard, 2021, Available: https://webstore.iec.ch/publication/64645.

[5] D. Systemes, “CST Studio Suite 3D EM Simulation and Analysis Software.” , Available: https://www.3ds.com/products-services/simulia/products/cst-studio-suite/.

[6] A. C. Marvin, G. Esposito, J. F. Dawson, I. D. Flintoft, L. Dawson, J. A. K. Everard, and G. C. R. Melia, “A Wide-Band Hybrid Antenna for Use in Reverberation Chambers,” in *Electromagnetic Compatibility (EMC), 2013 IEEE International Symposium On*, 2013, pp. 222–226, Available: http://eprints.whiterose.ac.uk/132442/.

[7] I. D. Flintoft, S. J. Bale, A. C. Marvin, M. Ye, J. F. Dawson, M. Z. Changyong Wan, S. L. Parker, and M. P. Robinson, “Representative Contents Design for Shielding Enclosure Qualification from 2 to 20 GHz,” *Electromagnetic Compatibility, IEEE Transactions on*, vol. 60, no. 1, pp. 173–181, Feb. 2018, Available: http://eprints.whiterose.ac.uk/116849/.